(Article begins on next page)

Journal Pre-proof

Development of antimicrobial films based on chitosan-polyvinyl alcohol blend enriched with ethyl lauroyl arginate (LAE) for food packaging applications

Hossein Haghighi, Serge Kameni Leugoue, Frank Pfeifer, Heinz Wilhelm Siesler, Fabio Licciardello, Patrizia Fava, Andrea Pulvirenti

Please cite this article as: Haghighi, H., Leugoue, S.K., Pfeifer, F., Siesler, H.W., Licciardello, F., Fava, P., Pulvirenti, A., Development of antimicrobial films based on chitosan-polyvinyl alcohol blend enriched with ethyl lauroyl arginate (LAE) for food packaging applications, *Food Hydrocolloids* (2019), doi: https://doi.org/10.1016/j.foodhyd.2019.105419.

This is a PDF file of an article that has undergone enhancements after acceptance, such as the addition of a cover page and metadata, and formatting for readability, but it is not yet the definitive version of record. This version will undergo additional copyediting, typesetting and review before it is published in its final form, but we are providing this version to give early visibility of the article. Please note that, during the production process, errors may be discovered which could affect the content, and all legal disclaimers that apply to the journal pertain.
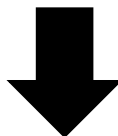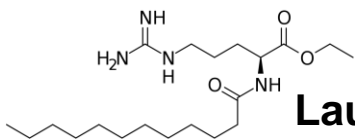
Chitosan (CS)
(1% w/v)

+
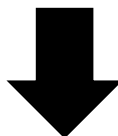
Polyvinyl Alcohol (PVA)
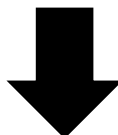(5% w/v)

CS-PVA Blend FFS
(1:1)

+

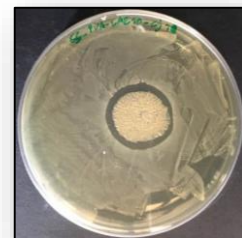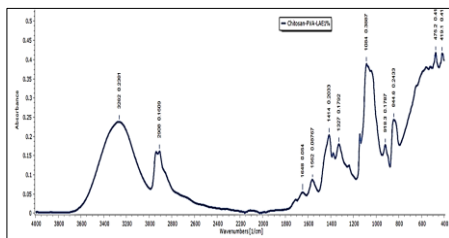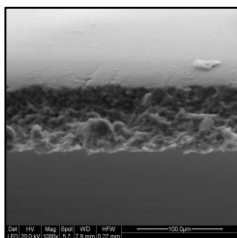**Lauroyl Arginate Ethyl (LAE)**
(1, 2.5, 5 and 10 % w/w)

CS-PVA-LAE Film

Characterization for Food Packaging Applications

(Microstructure, FT-IR, Thickness, Mechanical, Optical, Water Barrier and Antimicrobial Properties)

1 **Development of antimicrobial films based on chitosan-polyvinyl alcohol blend**

2 **enriched with ethyl lauroyl arginate (LAE) for food packaging applications**

3 Hossein Haghighi[a], Serge Kameni Leugoue[a,b], Frank Pfeifer[c], Heinz Wilhelm Siesler[c], Fabio

4 Licciardello[a,d,*], Patrizia Fava[a,d], Andrea Pulvirenti[a,d]

5 [a] Department of Life Sciences, University of Modena and Reggio Emilia, 42122, Reggio

6 Emilia, Italy

7 [b] Department of Zootechny, University of Dschang, 222, Dschang, Cameroon

8 [c] Department of Physical Chemistry, University of Duisburg-Essen, 45117, Essen, Germany

9 [d] Interdepartmental Research Centre BIOGEST-SITEIA, University of Modena and Reggio

10 Emilia, 42124, Reggio Emilia, Italy

11 [*] Corresponding author: fabio.licciardello@unimore.it

12 **Abstract**

13 The main aim of this study was to characterize microstructural, physical, optical, mechanical,

14 water barrier and antimicrobial properties of chitosan-polyvinyl alcohol blend films (CS-PVA)

15 enriched with ethyl lauroyl arginate (LAE) (1-10% w/v) for food packaging applications. The

16 film microstructure was determined by scanning electron microscopy. Active films containing

17 10% LAE showed cracks on the surface with irregular shape in the cross-section indicating a

18 weaker cohesion of the CS-PVA polymer blend at high LAE concentrations. The possible

19 interaction of CS-PVA blend film with incorporated LAE was also investigated using Fourier-

20 transform infrared (FT-IR) spectroscopy in the attenuated total reflection (ATR) mode. FT-

21 IR/ATR spectra showed a low molecular interaction between the CS-PVA and LAE up to

22 2.5% while for films containing 5 and 10% LAE such interactions between the functional

23 groups of the CS-PVA matrix and LAE have been detected. The active films were

24 transparent and showed barrier properties against UV and visible light. The incorporation of

25 LAE into the CS-PVA increased the thickness, water solubility, water vapor permeability, and

26 the b* and ΔE* values, while it decreased mechanical properties and transparency ($p < 0.05$).

27 Active films inhibited the growth of four major food bacterial pathogens including

28 *Campylobacter jejuni*, *Escherichia coli*, *Listeria monocytogenes* and *Salmonella typhimurium*.

29 Particularly, films containing 5 and 10% LAE were the most effective ($p<0.05$). Overall, the

30 characterization of functional properties revealed that CS-PVA blend film incorporated with

31 LAE could be used as an environmentally friendly antimicrobial packaging material to extend

32 the shelf life of food products.

33 **Keywords:** Active food packaging, ATR/FT-IR, Bio-based packaging, Ethyl lauroyl arginate

34 (LAE)

35 **1.   Introduction**

36 The current trend in food packaging is mainly oriented towards the substitution of non-

37 biodegradable petroleum-based polymers by packaging materials that are eco-friendly and

38 also prolong food shelf life (Kanatt, Rao, Chawla, & Sharma, 2012). In this context,

39 considerable research has been conducted involving the fabrication of biodegradable food

40 packaging materials that come from renewable natural resources and agri-food industry

41 wastes (Cazón, Vázquez, & Velazquez, 2018; Sarwar, Niazi, Jahan, Ahmad, & Hussain,

42 2018). Among bio-based natural polymers, chitosan (CS) has received significant attention

43 for its potential to substitute - partially or totally - petroleum-based polymers (Leceta,

44 Guerrero, & De La Caba, 2013). CS is a cationic linear polysaccharide consisting of poly-β-

45 (1–4)-D-glucosamine units obtained by partial deacetylation of chitin, the major component of

46 the insect's exoskeleton and shells of crustacean such as crab, shrimp, and crawfish. CS is

47 the second most abundant polysaccharide after cellulose with unique biological properties

48 such as biocompatibility, biodegradability and non-toxicity. In addition, this amino

49 polysaccharide has high antimicrobial activity against many pathogenic and spoilage

50 microorganisms, including both Gram-positive and Gram-negative bacteria which makes it an

51 excellent candidate for food packaging applications (Rubilar, Candia, Cobos, Díaz, &

52 Pedreschi, 2016). However, there are some limitations which are associated with CS such as

53 low mechanical strength, low thermal stability, rigid crystalline structure and high production

54 cost. A simple and effective alternative to overcome these drawbacks could be blending of

55 CS with synthetic polymers. Films formed by the blending of natural and synthetic polymers

56 represent a new class of material with modified physical and mechanical properties

57 compared to films made of individual components. Blending CS with polyvinyl alcohol (PVA)

58 has been intensively investigated by many researchers to gain biodegradable and

59 antimicrobial films for food packaging applications with new and desired properties (Bonilla,

60 Fortunati, Atarés, Chiralt, & Kenny, 2014; Kanatt et al., 2012; Liu, Wang, & Lan, 2018;

61 Tripathi, Mehrotra, & Dutta, 2009; Parida, Nayak, Binhani, & Nayak, 2011).

62 PVA is a synthetic, low cost, non-toxic and water-soluble polymer commercially obtainable

63 from hydrolysis of polyvinyl acetate with excellent film forming properties. Despite its

64 synthetic character, this polymer was recognized as biodegradable and it shows high tensile

65 strength, flexibility, gas barrier properties and good resistance to acid and alkali media (Aloui

66 et al., 2016). PVA has been evaluated for safety by the Joint FAO/WHO Expert Committee

67 on Food Additives (JECFA) in 2003 at the 61st meeting (Bellelli, Licciardello, Pulvirenti, &

68 Fava, 2018) and it has also been approved for use in packaging meat and poultry products

69 by the USDA (Kanatt et al., 2012). PVA is highly miscible with other hydrophilic polymers

70 such as CS, owing to the formation of intermolecular hydrogen bonds between hydroxyl

71 groups of PVA and hydroxyl and amine groups of CS. Due to the high compatibility of CS

72 and PVA, the resulting films show homogeneous structure. Moreover, blending PVA with CS

73 is a promising strategy to reduce the production cost and improve the mechanical property

74 and stability of CS films.

75 Antimicrobial packaging as a part of active packaging systems is intended to extend the shelf

76 life of food products and assure the safety and quality of packaged foods (Tripathi, Mehrotra,

77 & Dutta, 2008). Ethyl lauroyl arginate (LAE) is considered as an effective antimicrobial

78 substance among novel food additives (Rubilar et al., 2016). LAE remains stable at pH 3-7

79 and is odorless and colorless as well (Kashiri et al., 2016). LAE is a synthetic surfactant

80 consisting of an ethyl esterified arginine head with a lauroyl tail attached to the α-amino

81 group that is highly active against a wide range of food pathogens and spoilage

82 microorganisms including bacteria, yeast and molds with a low-dose application (Becerril,

83 Manso, Nerin, & Gómez-Lus, 2013). This cationic surfactant disrupts the cytoplasmic

84 membrane of microorganisms and inhibits the growth of microorganisms by causing cell

85   deformation and affecting their metabolic process negatively (Muriel-Galet, Carballo,

86   Hernández-Muñoz, & Gavara, 2016). LAE has been considered as GRAS (generally

87   recognized as safe) by the U.S. Food and Drug Administration (FDA, 2005) and has been

88   authorized as food preservative by the European Food Safety Authority (EFSA, 2007).

89   Incorporation of LAE as an antimicrobial compound into antimicrobial packaging to improve

90   food safety and quality has been reported in several studies (De Leo et al., 2018; Haghighi et

91   al., 2019a; Higueras, López-Carballo, Hernández-Muñoz, Gavara, & Rollini, 2013; Kashiri et

92   al., 2016; Moreno, Cárdenas, Atarés, & Chiralt, 2017a; Rubilar et al., 2016). However,

93   literature concerning the effects of LAE on the functional properties of CS-PVA blend film is

94   not available. Therefore, the objective of the present study was to develop biodegradable

95   films based on CS-PVA blend enriched with different concentrations of LAE to evaluate

96   microstructural, physical, optical, mechanical and water barrier properties for food packaging

97   applications. Moreover, the antimicrobial activity of films against four common food bacterial

98   pathogens including *Campylobacter jejuni*, *Escherichia coli*, *Listeria monocytogenes* and

99   *Salmonella typhimurium,* was investigated.

100   **2.   Material and methods**

101   *2.1   Materials and reagents*

102   Chitosan (CS) with a molecular weight of 100-300 kDa was obtained from Acros Organics[TM]

103   (China). Polyvinyl alcohol (PVA) with molecular weight of 27 kDa and 98% degree of

104   hydrolysis was purchased from Fluka (Steinheim, Germany). Glycerol (≥ 99.5%) was

105   purchased from Merck (Darmstadt, Germany). Acetic acid (≥ 99.5%) was obtained from

106   Brenntag S.p.A (Milan, Italy). Ethyl lauroyl arginate (LAE) was kindly provided as Mirenat-D

107   (69.3% LAE, 30.7% maltodextrin) by Vedeqsa Grupo LAMIRSA (Terrassa, Barcelona,

108   Spain). Brain heart infusion agar (BHIA) was purchased from Biolife (Milan, Italy).

109   *2.2.   Preparation of film-forming solutions (FFS) and films*

110   Preparation of films was adapted from the procedures of Higueras et al., (2013) and Kanatt

111   et al., (2012) with slight modification. In this study, four CS-PVA blend films enriched with

112   different concentrations of LAE (1, 2.5, 5 and 10% w/w of biopolymer) were analyzed.

113 Furthermore, a CS-PVA film-forming solution (FFS) without LAE was used to produce a

114 control film. The CS FFS (1%, w/w) was prepared by dissolving CS in an acetic acid solution

115 (1% v/v) under continuous stirring at 55°C for 60 min. The PVA FFS (5% w/w) was prepared

116 by dissolving PVA in distilled water at 80°C for 60 min. Glycerol (0.5% v/v of FFS) was then

117 added as a plasticizer into both FFSs, followed by additional stirring for 60 min. The CS-PVA

118 blend FFS was prepared by mixing CS and PVA FFSs at 1:1 ratio and final plasticizer

119 content was 17g glycerol/ 100 g dry polymer. Different amounts of LAE were added to the

120 CS-PVA blend FFS to obtain active films with 1-10% LAE (g of LAE/100 g of dry CS-PVA

121 blend) considering the LAE concentration (69.3%) in Mirenat-D. All FFSs were degasified

122 with a vacuum pump (70 kPa) for 15 min to remove bubbles. Films were obtained by casting

123 20 mL of the FFS into Petri dishes (14.4 cm in diameter) and drying at 25±2 °C in the

124 chemical hood overnight.

125 ### *2.3. Scanning electron microscopy (SEM)*

126 The SEM images from the surface and cross-section of the films were obtained with the use

127 of a scanning electron microscope (FEI, Quanta 200, Oregon, USA). Film samples were

128 fixed on a stainless-steel support with a double-sided conductive adhesive. The analysis was

129 conducted in low vacuum (0.6 Torr) at an acceleration voltage of 20 kV.

130 ### *2.4. Atomic force microscopy (AFM)*

131 The surface morphology of the films was analyzed using an atomic force microscope (Park

132 Scientific Instruments, South Korea). Films were fixed onto AFM specimen metal discs using

133 a double-sided tape and then placed to a magnetic sample holder located on the top of the

134 scanner tube. The images were scanned in no-contact mode under ambient condition. The

135 surface roughness (R_a) of the films was calculated on the basis of the root mean square (R_q)

136 deviation from the average height of peaks after subtracting the background using ProScan

137 software (version 1.51b). All samples were analyzed in triplicate.

138 ### *2.5 Attenuated Total Reflection (ATR) / Fourier-Transform Infrared (FT-IR)*

139 ### *Spectroscopy*

140 The infrared spectra of different films were obtained using an ATR/FT-IR spectrometer (type

141 Alpha, Bruker Optik GmbH, Ettlingen, Germany). Spectra were collected from two different

142 locations from the top and bottom side of the same samples in the 4000-400 cm^{-1}

143 wavenumber range by accumulating 64 scans with a spectral resolution of 4 cm^{-1}.

144 ### 2.6.   Thickness and mechanical properties

145 Film thickness was measured with a digital micrometer (Model IP65, SAMA Tools, Viareggio,

146 Italia) at five different random positions (one at the center and four at the edges). The means

147 of these five separate measurements were recorded.

148 The tensile strength (TS), elongation at break (E%) and elastic modulus (EM) were

149 determined using a dynamometer (Z1.0, Zwick/Roell, Ulm, Germany) according to ASTM

150 standard method D882 (ASTM, 2001a). The films with known thickness were cut into

151 rectangular strips (9.0 x 1.5 cm^2). Initial grip separation and cross-head speed were set at 70

152 mm and 50 mm/min, respectively. Measurements were repeated 10 times from each type of

153 film. The software TestXpert® II (V3.31) (Zwick/Roell, Ulm, Germany) was used to record the

154 TS curves. TS was calculated by dividing the maximum load to break the film by the cross-

155 sectional area of the film and expressed in MPa. The E% was calculated by dividing film

156 elongation at rupture by the initial grip separation expressed in percentage (%). EM was

157 calculated from the initial slope of the stress-strain curve and expressed in MPa.

158 ### 2.7.   UV barrier, light transmittance, opacity value and color

159 The barrier properties of films against UV and visible light were determined at the UV (200,

160 280 and 350 nm) and visible (400, 500, 600, 700 and 800 nm) wavelengths. These optical

161 characteristics were estimated with a VWR®Double Beam UV-VIS 6300PC

162 spectrophotometer (China) using square film samples (2 × 2 cm^2). The opacity of the films

163 was calculated by Eq. (1):

164 Opacity value$= \frac{-\log T\,600}{x}$ (1)

165 where T_{600} is the fractional transmittance at 600 nm and x is the film thickness (mm). The

166 greater opacity value represents the lower transparency of the film. For each film, four

167 readings were taken at different positions and average values were determined.

168   The color of films was measured with a CR-400 Minolta colorimeter (Minolta Camera, Co.,

169   Ltd., Osaka, Japan) at room temperature, with D65 illuminant and 10° observer angle. The

170   instrument was calibrated with a white standard (L* = 99.36, a* = -0.12, b* = -0.07) before

171   measurements. Results were expressed as L* (lightness), a* (red/green) and b* (yellow/blue)

172   parameters. The total color difference (ΔE^*) was calculated using the following Eq. (2):

173    $$\Delta E^* = \sqrt{[(\Delta L^*)^2 + (\Delta a^*)^2 + (\Delta b^*)^2]} \qquad (2)$$

174   where ΔL^*, Δa^* and Δb^* are the differences between the corresponding color parameter of the

175   samples and that of a standard white plate used as the film background. For each film, five

176   readings were taken at different positions and the average values were determined from the

177   top and bottom sides.

178   **2.8.**   **Moisture content and water solubility**

179   Moisture content (MC) of the films (2×2 cm^2) was determined as the percentage of weight

180   loss upon drying to constant weight (Md) in an oven at 105 ± 2 °C and the initial weight (Mw)

181   according to the following Eq. (3):

182    $$MC\ (\%): \frac{Mw\text{-}Md}{Mw} \times 100 \qquad (3)$$

183   The solubility of films (2×2 cm^2) in water was determined by drying to constant weight in an

184   air-circulating oven at 105 ± 2 °C (Wi) and then each film was immersed in 50 mL distilled

185   water at 25 °C following Gontard, Guilbert, & Cuq, (1992) with slight modifications. After 24 h,

186   the film samples were dripped and dried to constant weight at 105 ± 2 °C (Wf) to determine

187   the weight of dry matter which was not solubilized in water. The measurement of water

188   solubility (WS) was determined according to the following Eq. (4):

189    $$WS\ (\%): \frac{Wi\text{-}Wf}{Wi} \times 100 \qquad (4)$$

190   All measurements for MC and WS were made in triplicate.

191   **2.9.**   **Water vapor transmission rate and water vapor permeability**

192   Water vapor transmission rate (WVTR) of the films was determined gravimetrically in

193   triplicate according to the ASTM E96 method (ASTM, 2001b) with some modifications. Films

194   were sealed on top of glass test cups with an internal diameter of 10 mm and a depth of 55

195 mm filled with 2 g anhydrous $CaCl_2$ (0% RH). The cups were placed in desiccators containing

196 $BaCl_2$ (90% RH), which were maintained in incubators at 45 °C. WVTR was determined

197 using the weight gain of the cups and was recorded and plotted as a function of time. Cups

198 were weighed daily for 7 days to guarantee the steady state permeation. The slope of the

199 mass gain versus time was obtained by linear regression ($r^2 ≥ 0.99$). WVTR (g /day m^2) and

200 WVP (g mm/kPa day m^2) were calculated according to the following Eqs. (5) and (6):

201 $$WVTR = \frac{\Delta W}{\Delta t \times A} \qquad (5)$$

202 $$WVP = \frac{WVTR \times L}{\Delta P} \qquad (6)$$

203 where $\Delta W/\Delta t$ is the weight gain as a function of time (g/day), A is the area of the exposed

204 film surface (m^2), L is the mean film thickness (mm) and ΔP is the difference of vapor

205 pressure across the film (kPa).

206 ### 2.10. In vitro antimicrobial activity

207 ### 2.10.1. Disk diffusion assay

208 Antibacterial activity test on films was assessed against four typical food bacterial pathogens

209 including *Listeria monocytogenes* (UNIMORE 19115), *Escherichia coli* (UNIMORE 40522),

210 *Salmonella typhimurium* (UNIMORE 14028) and *Campylobacter jejuni* (UNIMORE 33250)

211 using the disk diffusion assay according to (Haghighi et al., 2019). Films (sterilized with UV

212 light) were cut into a disc shape of 22 mm diameter and placed on the surface of BHIA agar

213 plates, which had been previously streaked with 0.1 mL of inocula containing 10^6 CFU/mL of

214 tested bacteria. The plates were then incubated at 30 °C for 24 h (*C. jejuni* plates were

215 incubated at 37 °C). The diameter of the inhibition zones was measured with a caliper and

216 recorded in millimeters (mm). All tests were performed in triplicates.

217 ### 2.10.2. Evaluation of antimicrobial activity in liquid medium

218 Antimicrobial activity of CS-PVA films enriched with LAE (1-10%) evaluated against *L.*

219 *monocytogenes*, *E. coli*, *S. typhimurium* and *C. jejuni* in liquid medium (Kashiri et al., 2016).

220 A loop of each strain was transferred to 10 mL of BHIB and incubated at 30°C (*C. jejuni*

221 plates were incubated at 37 °C) for 24 h to obtain stationary phase (optical density of 0.9 at

222 600 nm). Then, cells were diluted in BHIB and incubated at 30 °C (*C. jejuni* tube was

223 incubated at 37 °C) to obtain exponential phase (optical density of 0.2 at 600 nm). One

224 hundred µL of microorganism in exponential phase was inoculated into tubes with 10 mL of

225 BHIB. A 0.025 g portion of film (1.5 x 1.5 cm^2) was added to each tube in sterile conditions.

226 The tubes were incubated at 30°C for 24 h. As a control, CS-PVA film without LAE was used.

227 Depending on the turbidity of each tubes, serial dilutions with NaCL were made and plated

228 on the Petri dishes with BHIA culture medium. Colonies were counted after incubation at 30

229 °C for 24 h.
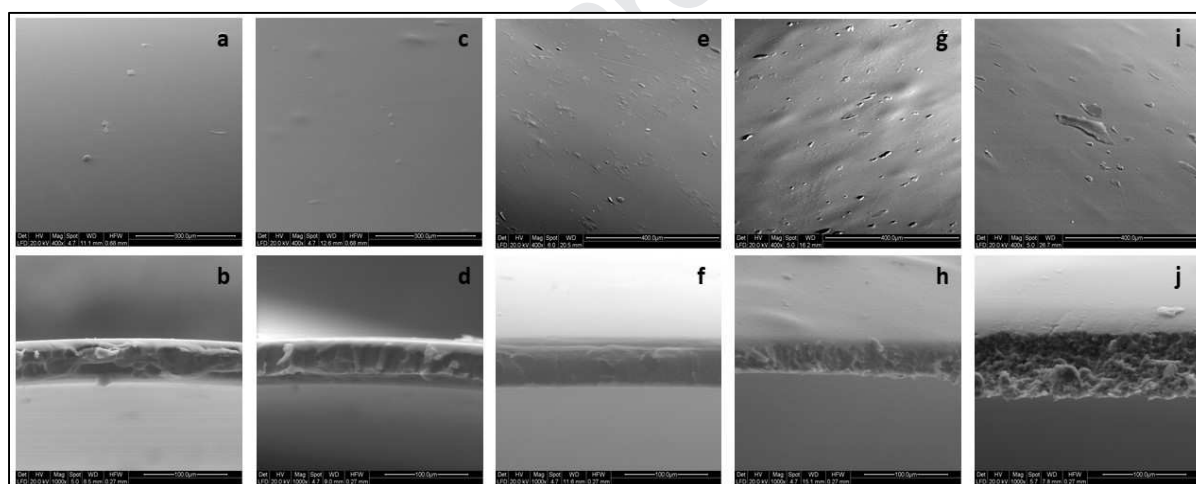
230 ### 2.10. Statistical analysis

231 The statistical analysis of the data was performed through analysis of variance (ANOVA)

232 using SPSS statistical program (SPSS 20 for Windows, SPSS INC., IBM, New York). The

233 experiment was performed in 3 replicates and the number of repeats varied from one

234 analysis to another and was reported in each subsection. The differences between means

235 were evaluated by Tukey's multiple range test ($p < 0.05$). The data were expressed as the

236 mean ± SD (standard deviation).

237 ## 3.   Results and discussion

238 ### 3.1.   Scanning electron microscopy (SEM)

239 The surface and cross-section images of CS-PVA blend film (control) and CS-PVA film

240 enriched with different concentrations of LAE (1-10%) (active films) are presented in Fig. 1.

241 The film microstructure greatly affects the final physical, mechanical and barrier properties.

242 This is mainly due to the interaction between the film components and LAE. The surface of

243 the control film was smooth and homogenous and did not show pores or cracks indicating

244 good compatibility between CS and PVA to form a blend (Fig. 1a). This could be explained

245 by strong molecular interaction between functional groups of chitosan and PVA. Similar

246 results were reported by Ghaderi, Hosseini, & Gómez-Guillén (2019) and Jahan, Mathad, &

247 Farheen (2016) who noticed that the surface of CS-PVA blend film was homogenous without

248 pores. Addition of LAE up to 1% did not affect the surface morphology of active films (Fig. 1c)

249 indicating LAE was evenly distributed and well dispersed in the film matrix. Small particles

250 and aggregations were observed at the surface of films with increasing concentration of LAE

251 up to 10% (Fig. 1e, 1g and 1i). A compact and continuous structure without irregularities like

252 air bubbles and pores and any evidence of phase separation can be observed in the cross-

253 section of the control film (Fig. 1b). The cross-section of active films containing LAE up to

254 2.5% showed similar results (Fig. 1d and 1f). However, active films containing 5 and10%

255 LAE showed irregular and sponge shape structure (Fig. 1h and 1j). This effect was more

256 obvious in CS-PVA film containing 10% LAE. This might be related to the agglomeration of

257 LAE in the film matrix at high concentrations which resulted in disrupted structures. The

258 interaction between the polymer chains was disturbed by interactions with functional groups

259 of LAE, producing films with less integrity. Gaikwad, Lee, Lee, & Lee (2017) also reported

260 that the order of low-density polyethylene (LDPE) films was interrupted by the addition of

261 high amount of LAE powder (5 and 10%) mainly due to the inhomogeneous distribution of

262 LAE inside the matrix and the low interfacial interaction between the LDPE and LAE powder.

263
264 **Fig. 1**. Scanning electron microscopy (SEM) images of the surface and cross-section of films
265 based on a control CS-PVA blend (CS-PVA) (a and b), CS-PVA-LAE1% (c and d), CS-PVA-
266 LAE2.5% (e and f), CS-PVA-LAE5% (g and h) and CS-PVA-LAE10% (i and j).
267

3.2. *Atomic force microscopy (AFM)*

269 AFM was further performed to characterize the surface morphology of control and active

270 films. Typical 3D surface topographic AFM images and root mean square (R_q) and

271 roughness (R_a) values are presented in Fig. 2. The surface of control film was relatively

272 smooth and homogenous as indicated by lower R_q and R_a values (17.1 and 12.0 nm,

273 respectively). Increasing concentration of LAE up to 10% led to the increase in the

274 roughness of the films, as indicated by higher R_q and R_a values. The difference in roughness

275   value between control and active films was in accordance with the film microstructure

276   observed by SEM analysis.

277

278
279   **Fig. 2**. 3D AFM images, root mean square (R_q) and roughness (R_a) of films based on a:
280   control CS-PVA blend, b: CS-PVA-LAE 1%, c: CS-PVA-LAE 2.5%, d: CS-PVA-LAE 5% and
281   e: CS-PVA-LAE 10%.
282

3.3.   Attenuated Total Reflection (ATR) / Fourier-Transform Infrared (FT-IR)

Spectroscopy

285   ATR/FT-IR spectroscopy was performed to characterize the structural and spectroscopic

286   changes due to the incorporation of different amounts of LAE (1-10% w/w) into the CS-PVA

287   film matrix by measuring the spectra in the wavenumber range of 4000-400 cm^{-1} at a

288   spectral resolution of 4 cm^{-1}. The spectrum of the control CS-PVA blend (Fig. 3A, a) revealed

289   the characteristic bands of the two polymer components (CS and PVA) with relative

290   intensities according to the respective composition. Under the broad and intense absorption

291   band with the maximum at about 3270 cm^{-1}, the ν(OH), ν(NH) and ν_{as}(NH$_2$)/ν_s(NH$_2$)

292   absorption bands of these inter- and intramolecularly hydrogen bonded functionality of the

293   CS and PVA blend components are superimposed (Costa-junior, Pereira, & Mansur, 2009;

294   Kumar, Krishnakumar, Sobral, & Koh, 2019). The neighboring band doublet at about

295   2937/2908 cm^{-1} can be assigned to antisymmetric and symmetric ν_{as}(CH$_2$)/ν_s(CH$_2$) and

296   ν(CH) stretching vibrations of the corresponding polymer chain functionalities (Liu et al.,

297   2018). Characteristic absorption bands for CS can be assigned at 1646 cm^{-1} (amide-I) due to

298 the ν(C=O) stretching vibration, and at 1561 cm^{-1} (amide II) to a combination band of the

299 ν(C–N) stretching and δ(N-H) bending vibrations (Costa-junior et al., 2009). Because in this

300 study a PVA with only 98% degree of hydrolysis was used, 2% of acetate groups remained

301 non-hydrolyzed during the manufacturing process (Koosha & Mirzadeh, 2015). Thus, the

302 band at 1708 cm^{-1} belongs to the ν(C=O) stretching vibration of residual vinyl acetate units in

303 the PVA backbone (Costa-junior et al., 2009). The very sharp, crystallinity-sensitive band of

304 PVA at 1140 cm^{-1} is also observed in the CS-PVA blend (Kim, Kim, Lee, & Kim, 1992;

305 Tripathi et al., 2009). Furthermore, absorption bands at 1413 cm^{-1} (δ(CH$_2$) bending

306 vibration), between 1085 and 1045 cm^{-1} (ν(C–O) stretching vibrations), and 917 cm^{-1} (CH$_2$

307 rocking vibration) can be observed in the ATR/FT-IR spectrum of the CS-PVA blend

308 (Pavaloiu, Stoica-Guzun, Stroescu, Jinga, & Dobre, 2014; Pereira Jr, de Arruda, & Stefani,

309 2015). For a better visualization and understanding of the – although minor – spectral

310 changes in the wavenumber ranges 2800 – 3000 cm^{-1} and specifically 1500 – 1800 cm^{-1} (see

311 Fig. 3B) upon addition of LAE to the CS-PVA blends, the spectrum of pure Mirenat-D is

312 reproduced in Fig.4. The most important absorption bands of the spectral range between

313 1000 and 3500 cm^{-1} can be readily assigned to the different vibrations of the chemical

314 building blocks of this additive.

315 Up to 2.5% LAE content, the characteristic absorption bands in the ATR/FT-IR spectra of the

316 CS-PVA blends (Fig. 3A, b and c) are wavenumber invariant and do not show intensity

317 changes, thereby suggesting low molecular interaction between the polymer and the LAE.

318 Similar results were reported by Gaikwad, Lee, Lee, & Lee (2017); Rubilar et al. (2016) and

319 Kashiri et al. (2016). However, CS-PVA blend films containing 5% and 10% LAE (Fig. 3A, d

320 and e) revealed new absorption bands at 2918 cm^{-1} and 2851 cm^{-1} (ν_{as}(CH$_2$)/ν_s(CH$_2$)), 1755

321 cm^{-1} (ν(C=O)), 1724 cm^{-1} (ν(C=O)) and 1661/1645 cm^{-1} (ν(C=O), ν(C=N), δ(NH$_2$)) originating

322 from the introduction of new CH$_2$-segments, ester, amide, NH$_2$ and imine groups (Gamarra,

323 Missagia, Urpí, Morató, & Muñoz-Guerra, 2018; Moreno et al., 2017a). The evolution of the

324 band doublet (1661/1645 cm^{-1}) from the original 1646 cm^{-1} band and the shift of the 1561 cm^{-}

325 ^{1} band to 1557 cm^{-1} (LAE 5%) and to 1544 cm^{-1} (LAE 10%), respectively (Fig. 3B, d and e), is

326 a clear evidence, that at elevated LAE content the C=O, NH_2 and NH functionalities of this

327 additive contribute to competitive intermolecular interactions with the hydroxyl, amino, ether

328 and residual acetate groups of the CS-PVA film network. Furthermore, LAE can also promote

329 the formation of C=N groups, by reacting with both, residual acetate carbonyls of PVA and

330 CS amino groups, as revealed by the relative intensity of the peak at 1645 cm^{-1} for LAE 10%

331 (Fig 3B, e). Thus, the carbonyl-amino reaction to form C=N groups was enhanced by the

332 presence of LAE (Moreno et al., 2017a).

333
334 **Fig. 3.** ATR/FT-IR spectra (A) of films based on a: control CS-PVA blend, b: CS-PVA-LAE
335 1%, c: CS-PVA-LAE 2.5%, d: CS-PVA-LAE 5% films and e: CS-PVA-LAE 10%. In (B) the
336 enlarged 1800-1500 cm^{-1} region is shown to highlight the spectral changes at elevated LAE
337 content.

Fig. 4. ATR/FT-IR spectra of LAE formulation (Mirenat-D).

3.4. Thickness

The thickness value is a crucial parameter for determining final physical, mechanical and barrier properties of biodegradable films. The thickness values of control and active films are reported in Tab. 1. Thickness values ranged from 44.81 to 59.82 µm. The control film showed the lowest value ($p < 0.05$). This is due to the well-organized and dense network structure in the CS-PVA blend film as confirmed by SEM images. The incorporation of LAE into the CS-PVA blend increased the thickness ($p < 0.05$) and the CS-PVA film enriched with 10% LAE showed the highest thickness value ($p < 0.05$). In this study, all films were prepared by casting a constant amount of FFS in Petri dishes with the same surface ratio, therefore differences in thickness between control and active films are due to the addition of LAE to the FFS. According to Gaikwad et al. (2017), film thickness is influenced by the solid content of the FFS. Thus, LAE might contribute to loosen film matrix, reduce the homogeneity, and consequently increase the thickness. In contrast, Rubilar et al., (2016) reported that addition of LAE to CS films did not influence the thickness. It is noteworthy that the type of LAE applied in different studies as a powder (Mirenat-D or Mirenat-P) or dissolved in glycerol (Mirenat-G) strongly affects film thickness.

3.5. Mechanical properties

358   The tensile strength (TS), elongation at break (E%) and elastic modulus (EM) are three

359   important parameters for evaluation of mechanical properties. Generally, adequate

360   mechanical strength and extensibility are required for the development of biodegradable films

361   for food packaging applications. The mechanical properties of control and active films are

362   presented in Tab. 1. The control film showed the highest TS, E% and EM values. The

363   presence of LAE greatly influenced TS and E% ($p<0.05$). Films containing LAE were less

364   resistant and less stretchable than the control film ($p<0.05$). Incorporation of LAE up to 10%

365   decreased the tensile strength from 42.48 to 15.70 MPa and E% from 54.25 to 14.31%. The

366   significant deterioration of mechanical properties above 2.5% incorporation of LAE (Tab. 1) is

367   also consistent with the ATR/FT-IR observation, that band shifts and intensity changes occur

368   above this threshold concentration. This tendency could be explained by the fact that active

369   films containing a high concentration of LAE are unable to form a cohesive and continuous

370   matrix as it was confirmed by SEM analysis. This can be attributed to the competitive

371   interaction of the functional groups of LAE and the CS-PVA blend that limit cohesion forces

372   within the polymer in the film matrix and consequently decrease the degree of physical

373   crosslinking by weakening the intermolecular hydrogen bonding, thereby resulting in the

374   reduction of mechanical properties. Despite the reduction of TS after incorporation of LAE, it

375   should be noted that the TS values for the active films containing LAE up to 2.5% were

376   comparable with those of plastic films that are used widely in the market, such as high

377   density polyethylene (22-31 MPa) and polypropylene (31-38 MPa) but slightly lower than that

378   for polystyrene (45-83 MPa) (Theinsathid, Visessanguan, Kruenate, Kingcha, & Keeratipibul,

379   2012). Moreno, Díaz, Atarés, & Chiralt (2016) also reported that the incorporation of LAE into

380   starch-gelatin blend film notably reduced the stiffness and resistance to break compared to

381   the control film. In contrast to these results, Rubilar et al. (2016) reported that the

382   incorporation of LAE (1g/L) to CS films significantly increased TS and E% values ($p<0.05$)

383   which might be due to the application of Mirenat-G (10% LAE, 90% glycerol) as LAE source.

384   Hence the observed effect could be mainly due to the plasticizing effect of glycerol. Literature

385   data regarding mechanical properties are controversial and are influenced by multiple factors

386 such as the molecular mass of the polymer, deacetylation degree of CS, degree of hydrolysis

387 of PVA, pH of the FFS, drying conditions and type of LAE.

388 **Table 1**
389 Thickness, tensile strength (TS), elongation at break (E%) and elastic modulus (EM) of the
390 films based on control CS-PVA blend (CS-PVA) and CS-PVA enriched with LAE (1-10%
391 w/w).

Film sample	Thickness (µm)	TS (MPa)	E (%)	EM (MPa)
CS-PVA	44.8 ± 1.0[a]	42.5 ± 1.6[d]	54.2 ± 2.0[d]	1570.1 ± 139.0[d]
CS-PVA-LAE 1%	45.1 ± 0.5[a]	33.0 ± 2.4[c]	38.9 ± 3.1[c]	1153.1 ± 121.1[bc]
CS-PVA-LAE 2.5%	49.9 ± 1.6[b]	34.5 ± 4.2[c]	39.0 ± 2.6[c]	1287.3 ± 77.8[c]
CS-PVA-LAE 5%	54.9 ± 2.7[c]	22.2 ± 0.9[b]	25.0 ± 2.8[b]	1016.9 ± 90.8[b]
CS-PVA-LAE 10%	59.6 ± 0.8[d]	15.7 ± 1.2[a]	14.3 ± 1.9[a]	701.3 ± 53.8[a]

392 Values are given as mean ± SD (n = 3).
393 Different letters in the same column indicate significant differences ($p < 0.05$).

394 ### 3.6.   UV barrier, light transmittance and opacity value

395 Protecting food from the effect of UV-Vis radiation is one of the desired characteristics of

396 packaging material due to their influence on product performance and consumer acceptance.

397 The UV-Vis light transmittance of control and active films in the wavelength range of 200–

398 800 nm is presented in Fig. 5. Control film showed a higher UV light transmittance (200–350

399 nm) compared to the active films. UV light transmittance was reduced at increasing LAE

400 concentration and active films behaved as effective UV barriers at 200 nm since the

401 transmittance value was below 1%. UV barrier property of films is an important parameter for

402 food packaging applications to minimize UV-induced lipid oxidation, to preserve the

403 organoleptic properties of the packaged food, to avoid nutrient losses, discoloration and off-

404 flavors, thereby prolonging food shelf life (Hajji et al., 2016; Wu, Sun, Guo, Ge, & Zhang,

405 2017).

406 The transmission of visible light (400–800 nm) was higher than 80% for the control film. The

407 active films containing 1 and 2.5% LAE showed similar results while active films containing 5

408 and 10% LAE showed lower values. Thus, once a critical LAE concentration is exceeded,

409 aggregates are formed, that were large enough to scatter the light and thereby interfere with

410   its transmission (Bonnaud, Weiss, & McClements, 2010). The light barrier property is also an

411   important factor for food preservation to avoid photo-oxidation of organic compounds and

412   degradation of vitamins and other pigments. In addition, it provides a clear view of the food

413   content and its condition (Figueroa-Lopez, Andrade-Mahecha, & Torres-Vargas, 2018;

414   Yadav & Chiu, 2019). In this study, all films can be considered as transparent due to the

415   opacity value lower than 5 at 600 nm (Tab. 2). The higher value of this parameter represents

416   the lower transparency of the film.

417
418   **Fig. 5.** UV-Vis light transmittance of the films based on a control CS-PVA blend (CS-PVA)
419   and CS-PVA blends enriched with LAE (1-10% w/w).
420
421   ***3.7.   Color***

422   The color values (L*, a* and b*) and total color difference (ΔE*) of control and active films are

423   shown in Tab. 2. The L*, a*, b* offer objective evaluation of the appearance of films while

424   ΔE* measures the color change of treatment from a reference color. Color is an important

425   feature of a film for food packaging applications since it evaluates the visual characteristic of

426   the food product inside the packaging system and affects consumer purchase decision. The

427   L* value indicates lightness and represents the apparent proportion of incident light reflected

428   by an object, varying between 98.22 and 98.99, which means that all the films were almost

429   clear. No significant differences ($p > 0.05$) for L* between the control and active films were

430   found. These results were in agreement with opacity values that showed all films were clear

431   and transparent. The a* value, expressing the green-red color component, was negative for

432 all films, which means that films were not truly red (Virginia Muriel-Galet, López-Carballo,

433 Hernández-Muñoz, & Gavara, 2014). The b* value measures the blue-yellow color

434 component. This value increased upon addition of LAE (p<0.05), suggesting a gain of slight

435 yellow color. ΔE* was used to compare the color of active films with commercial plastic films

436 (perceptibility threshold of ΔE* = 1). The selected value is often used as the smallest color

437 difference that the human eye can detect (Thakhiew, Devahastin, & Soponronnarit, 2013).

438 Control film had ΔE* value of 0.91. The ΔE* increased upon addition of LAE (p<0.05) and

439 reached a value of 1.70 in the active film containing 10% LAE. This behavior might be

440 attributed to the increase in the colorimetric coordinate b* and increase in film thickness upon

441 addition of LAE. In summary, the consumer might not be able to detect color difference in

442 active films, despite the slightly higher values than the threshold. A similar result has been

443 reported by Rubilar et al. (2016).

444 **Table 2**
445 Color parameters (L*, a* and b*), total color difference (ΔE*) and opacity values of the films
446 based on a control CS-PVA blend (CS-PVA) and CS-PVA enriched with LAE (1-10% w/w).

Film sample	Color parameters				Opacity value
	L*	a*	b*	ΔE*	(600 nm)
CS-PVA	99.0 ± 0.2[a]	-0.3 ± 0.03[c]	0.7 ± 0.1[a]	0.91 ± 0.2[a]	0.9 ± 0.01[a]
CS-PVA-LAE 1%	98.8 ± 0.1[a]	-0.3 ± 0.01[c]	0.7 ± 0.1[a]	0.99 ± 0.1[a]	1.1 ± 0.08[ab]
CS-PVA-LAE 2.5%	98.8 ± 0.1[a]	-0.4 ± 0.02[b]	1.0 ± 0.1[b]	1.22 ± 0.1[b]	1.6 ± 0.31[bc]
CS-PVA-LAE 5%	98.6 ± 0.1[a]	-0.4 ± 0.03[a]	1.3 ± 0.2[c]	1.63 ± 0.2[c]	2.0 ± 0.13[c]
CS-PVA-LAE 10%	98.7 ± 0.2[a]	-0.5 ± 0.02[a]	1.4 ± 0.1[c]	1.70 ± 0.1[c]	3.1 ± 0.27[d]

447 Values are given as mean ± SD (n = 3).
448 Different letters in the same column indicate significant differences (p<0.05).

449 *3.8.   Moisture content, water solubility, water vapor transmission rate and water*

450 *vapor permeability*

451 One of the major drawbacks of biodegradable films for food packaging applications is their

452 sensitivity to water. Due to the hydrophilic nature of CS and PVA, when these films are

453 exposed to high relative humidity conditions, water molecules are absorbed by the polymeric

454 chains, exerting a plasticizing effect and resulting in changes of the mechanical and barrier

455 properties (Aguirre-Loredo, Rodríguez-Hernández, Morales-Sánchez, Gómez-Aldapa, &

456 Velazquez, 2016). Therefore, measuring water sensitivity plays an important role in the

457 packaging performance for the food products. The moisture content (MC), water solubility

458 (WS), water vapor transmission rate (WVTR) and water vapor permeability (WVP) of control

459 and active films are presented in Tab. 3.

460 The MC value ranged from 16.42 to 17.53%. The effect of LAE incorporation on the MC was

461 not significant (p<0.05). Moreno, Gil, Atarés, & Chiralt (2017b) reported that the enrichment

462 of starch-gelatin films with different LAE concentrations did not influence the MC. Solubility is

463 defined as the content of dry matter solubilized after 24 h immersion in water. The control

464 film showed the lowest WS value and addition of LAE increased the WS value. CS-PVA film

465 containing 10% LAE showed the highest WS value (p<0.05). The higher solubility values of

466 active films could be explained by the hydrophilic nature of CS-PVA blend film and low oil-

467 water equilibrium partition coefficient of LAE ($K_{ow}<0.1$), which means that LAE has a high

468 affinity to water molecules (Higueras et al., 2013; Rubilar et al., 2016).

469 The barrier properties of biodegradable films to water play an important role in determining

470 the shelf life of packed foodstuffs (Del Nobile, Fava, & Piergiovanni, 2002). In this study, the

471 WVTR was not significantly influenced by the addition of LAE, despite showing higher values

472 in active films (p>0.05). However, the incorporation of LAE to CS-PVA blend film increased

473 the WVP value. This might be due to the difference in each film thickness considered in WVP

474 calculation (Rubilar et al., 2016). Additionally, incorporation of LAE into the CS-PVA film

475 network may break hydrogen bonding and disrupt the long-range ordering between CS and

476 PVA molecules, resulting in an increase in WVP value (Ma, Zhang, & Zhong, 2016).

477 **Table 3**
478 Moisture content (MC), water solubility (WS), water vapor transmission rate (WVTR) and
479 water vapor permeability (WVP) of the films based on a control CS-PVA blend (CS-PVA) and
480 CS-PVA enriched with LAE (1-10% w/w).

Film sample	MC (%)	WS (%)	WVTR (g /day m^2)	WVP 90:0% RH (g mm/kP day m^2)
CS-PVA	16.4 ± 0.5[a]	22.1 ± 0.4[a]	3605.6 ± 450.8[a]	18 ± 0.02[a]
CS-PVA-LAE 1%	16.7 ± 0.9[a]	23.7 ± 2.8[ab]	3608.7 ± 362.1[a]	19 ± 0.02[a]

CS-PVA-LAE 2.5%	16.8 ± 0.7[a]	25.4 ± 3.4[ab]	3729.5 ± 369.3[a]	21 ± 0.02[ab]
CS-PVA-LAE 5%	17.1 ± 0.6[a]	27.8 ± 2.1[b]	3742.1 ± 341.5[a]	24 ± 0.02[b]
CS-PVA-LAE 10%	17.5 ± 0.6[a]	33.2 ± 2.1[c]	3808.9 ± 337.7[a]	26 ± 0.02[c]

481 Values are given as mean ± SD (n = 3).
482 Different letters in the same column indicate significant differences (p<0.05).

3.9. In vitro antimicrobial activity

3.9.1. Disk diffusion assay

485 The antimicrobial activity of control and active films against common bacterial food
486 pathogens, namely *C. jejuni*, *E. coli*, *L. monocytogenes* and *S. typhimurium*, was evaluated
487 by the disk diffusion assay (Fig. 6) and the details are presented in Tab. 4. The control film
488 did not show an inhibition zone against any of the tested microorganisms. The absence of
489 inhibition zone could be explained by the limitation of CS to diffuse in agar medium (Leceta,
490 Guerrero, Ibarburu, Dueñas, & De La Caba, 2013) and incapability of PVA to inhibit bacterial
491 growth as it has been reported by other authors (Hajji et al., 2016; Tripathi et al., 2009), so
492 that only microorganisms in direct contact with the active sites of CS in the CS-PVA film
493 network are inhibited. Active films containing 1% LAE were only effective against *C. jejuni*. In
494 general, LAE was more effective against *C. jejuni* compared to the other microorganisms
495 considered, which showed inhibition haloes ranging from 3 to 5-fold wider. No differences
496 were observed in the inhibition zones produced by CS-PVA films incorporating 5 and 10% of
497 LAE against all tested microorganisms. Similar results reported by Muriel-Galet, López-
498 Carballo, Gavara, & Hernández-Muñoz (2015). Pattanayaiying, H-Kittikun, & Cutter (2015)
499 also found that incorporation of LAE into pullulan film inhibited the growth of foodborne
500 pathogens such as *Salmonella spp.*, *L. monocytogenes* and *E. coli.* The antimicrobial activity
501 of LAE is attributed to its action as a cationic surfactant on the cytoplasmic membranes of
502 microorganisms, causing a disturbance in membrane potential and resulting in cell growth
503 inhibition and loss of viability (Kashiri et al., 2016; Muriel-Galet, López-Carballo, Gavara, &
504 Hernández-Muñoz, 2012).

505 **Table 4**
506 Inhibition zone diameters of the film disks (22 mm diameter) based on a control CS-PVA
507 blend (CS-PVA) and CS-PVA enriched with LAE (1-10% w/w).

Film sample	*L. monocytogenes*	*E. coli*	*C. jejuni*	*S. typhimurium*
CS-PVA	N. D.	N. D.	N. D.	N. D.
CS-PVA-LAE 1%	N. D.	N. D.	1.8 ± 1.0^{aA}	N. D.
CS-PVA-LAE 2.5%	0.5 ± 0.5^{aA}	0.6 ± 0.3^{aA}	3.7 ± 1.5^{bB}	0.6 ± 0.7^{aA}
CS-PVA-LAE 5%	1.3 ± 0.7^{abA}	1.2 ± 0.9^{abA}	4.6 ± 1.8^{bB}	1.7 ± 1.1^{abA}
CS-PVA-LAE 10%	1.6 ± 0.9^{bA}	1.6 ± 1.0^{bA}	5.2 ± 1.4^{bB}	1.8 ± 1.8^{aA}

508 Values are given as mean ± SD (n = 3). N.D: not detected.
509 Different lowercase letters in the same column indicate significant differences ($p<0.05$).
510 Different capital letters in the same row indicate significant differences ($p<0.05$).
511

512
513 **Fig. 6.** Disk diffusion results of films based on a control CS-PVA blend (CS-PVA) and CS-
514 PVA enriched with LAE (1-10% w/w).
515
3.9.2. Evaluation of antimicrobial activity in liquid medium

517 The Antimicrobial activity of control and active films against common bacterial food

518 pathogens including *C. jejuni*, *E. coli*, *L. monocytogenes* and *S. typhimurium* was also

519 evaluated in liquid medium and the details are presented in Tab. 5. CS-PVA film without LAE

520 used as a control. Among tested microorganisms *C. jejuni* showed higher log reduction (2)

521 for CS-PVA-LAE 10% films that is in agreement with the DDA result. The incorporation of

522 LAE (1-10%) showed a log reduction against all tested microorganisms. Clearly, the higher

523 the LAE concentration in the film, the greater the antimicrobial efficiency of the CS-PVA film.

524 Similar result were reported by (V. Muriel-Galet et al., 2015) and (Kashiri et al., 2016).

525 **Table 5**
526 Antimicrobial activity of films based on a control CS-PVA blend (CS-PVA) and CS-PVA
527 enriched with LAE (1- 10% w/w) expressed as logarithm of colony forming units (log CFU/
528 mL) and log reduction value (LRV).

Film sample	*L. monocytogenes*		*E. coli*		*C. jejuni*		*S. typhimurium*	
	log (cfu/mL)	*LRV*	*log (cfu/mL)*	*LRV*	*log (cfu/mL)*	*LRV*	*log (cfu/mL)*	*LRV*
CS-PVA	9.2 ± 0.2^b		9.3 ± 0.1^c		9.4 ± 0.1^b		9.5 ± 0.1^c	
CS-PVA-LAE1%	9.2 ± 0.2^b	0	9.1 ± 0.1^{bc}	0.2	9.2 ± 0.1^b	0.2	9.4 ± 0.1^{bc}	0.1
CS-PVA-LAE2.5%	9.0 ± 0.2^b	0.2	9.0 ± 0.1^{bc}	0.3	9.1 ± 0.3^b	0.3	9.3 ± 0.1^{bc}	0.2
CS-PVA-LAE5%	8.9 ± 0.2^b	0.3	8.8 ± 0.1^b	0.5	8.8 ± 0.1^b	0.6	9.2 ± 0.1^{ab}	0.3
CS-PVA-LAE10%	7.7 ± 0.8^a	1.5	8.3 ± 0.4^a	1	7.4 ± 0.1^a	2	9.1 ± 0.1^a	0.4

529 Values are given as mean ± SD (n = 3).
530 Different lowercase letters in the same column indicate significant differences (p<0.05).
531
532 **4.   Conclusion**

533 In this study, biodegradable active films based on CS-PVA blends enriched with LAE at

534 different concentrations (1-10%, w/w) were developed and their microstructural, physical,

535 optical, mechanical, barrier and antimicrobial properties were evaluated for food packaging

536 applications. The results showed that all films containing LAE were transparent. The

537 incorporation of LAE could improve the UV and light barrier properties of CS-PVA film, which

538 may be useful to protect food from UV degradation and photo-oxidation. The characteristic

539 absorption bands in the ATR/FT-IR spectra of the CS-PVA blends did not show significant

540 band shifts and intensity changes up to 2.5% LAE content, indicating low interactions

541 between the polymer and the LAE. However, at elevated LAE content the C=O, NH_2 and NH

542 functionalities of this additive contribute to competitive molecular interactions with the

543 hydroxyl, amino, ether and residual acetate groups of the CS-PVA film network. The

544 presence of LAE greatly influenced TS and E%. Films with LAE were less resistant and less

545 stretchable than the control film and a significant deterioration of mechanical properties

546 occurred above 2.5% incorporation of LAE. The developed active films, especially those

547 including 5 and 10% LAE, were effective against common bacterial food pathogens. The

548 results suggest that the CS-PVA films enriched with different concentrations of LAE could be

549 considered as environmentally friendly packaging material with antimicrobial properties to

550 extend the shelf life of food products and that might be an alternative to synthetic plastics for

551 certain applications.

552 **Declaration of interest**

553 None.

554 **Acknowledgements**

555 The authors would like to thank Dr. Massimo Tonelli and Centro Interdipartimentale Grandi

556 Strumenti (CIGS) of the University of Modena and Reggio Emilia for assistance in the SEM

557 and AFM measurements.

558 **References**

559 1. Aguirre-Loredo, R. Y., Rodríguez-Hernández, A. I., Morales-Sánchez, E., Gómez-

560   Aldapa, C. A., & Velazquez, G. (2016). Effect of equilibrium moisture content on

561   barrier, mechanical and thermal properties of chitosan films. *Food Chemistry*, *196*,

562   560–566. https://doi.org/10.1016/j.foodchem.2015.09.065

563 2. Aloui, H., Khwaldia, K., Hamdi, M., Fortunati, E., Kenny, J. M., Buonocore, G. G., &

564   Lavorgna, M. (2016). Synergistic effect of halloysite and cellulose nanocrystals on the

565   functional properties of PVA based nanocomposites. *ACS Sustainable Chemistry and

566   Engineering*, *4*(3), 794–800. https://doi.org/10.1021/acssuschemeng.5b00806

567 3. ASTM. (2001a). Standard test method for tensile properties of thin plastic sheeting. In

568   *Annual books of ASTM standards. Designation D882-01. Philadelphia: ASTM,

569   American Society for Testing Materials.*

570 4. ASTM. (2001b). Standard test method for water vapor transmission of materials. In

571 *Annual books of ASTM Standards. Designation E 96-01, Philadelphia: ASTM,*

572 *American Society for Testing Materials*

573 5. Becerril, R., Manso, S., Nerin, C., & Gómez-Lus, R. (2013). Antimicrobial activity of

574 Lauroyl Arginate Ethyl (LAE), against selected food-borne bacteria. *Food Control*,

575 *32*(2), 404–408. https://doi.org/10.1016/j.foodcont.2013.01.003

576 6. Bellelli, M., Licciardello, F., Pulvirenti, A., & Fava, P. (2018). Properties of poly(vinyl

577 alcohol) films as determined by thermal curing and addition of polyfunctional organic

578 acids.   *Food   Packaging   and   Shelf   Life*,   *18*,   95–100.

579 https://doi.org/10.1016/j.fpsl.2018.10.004

580 7. Bonilla, J., Fortunati, E., Atarés, L., Chiralt, A., & Kenny, J. M. (2014). Physical,

581 structural and antimicrobial properties of poly vinyl alcohol- chitosan biodegradable

582 films.   *Food   Hydrocolloids*,   *35*,   463–470.

583 https://doi.org/10.1016/j.foodhyd.2013.07.002

584 8. Bonnaud, M., Weiss, J., & McClements, D. J. (2010). Interaction of a food-grade

585 cationic surfactant (Lauric Arginate) with food-grade biopolymers (pectin,

586 carrageenan, xanthan, alginate, dextran, and chitosan). *Journal of Agricultural and*

587 *Food Chemistry, 58*(17), 9770–9777. https://doi.org/10.1021/jf101309h

588 9. Cazón, P., Vázquez, M., & Velazquez, G. (2018). Composite films of regenerate

589 cellulose with chitosan and polyvinyl alcohol: Evaluation of water adsorption,

590 mechanical and optical properties. *International Journal of Biological*

591 *Macromolecules, 117*, 235–246. https://doi.org/10.1016/j.ijbiomac.2018.05.148

592 10. Costa-junior, E. D. S., Pereira, M. M., & Mansur, H. S. (2009). Properties and

593 biocompatibility of chitosan films modified by blending with PVA and chemically

594 crosslinked. *Journal of Materials Science: Materials in Medicine, 20*(2), 553–561.

595 https://doi.org/10.1007/s10856-008-3627-7

596 11. De Leo, R., Quartieri, A., Haghighi, H., Gigliano, S., Bedin, E., & Pulvirenti, A. (2018).

597 Application of pectin-alginate and pectin-alginate-lauroyl arginate ethyl coatings to

598 eliminate Salmonella enteritidis cross contamination in egg shells. *Journal of Food*

599   *Safety*, *38*(6) 1-9. https://doi.org/10.1111/jfs.12567

600   12. Del Nobile, M. A., Fava, P., & Piergiovanni, L. (2002). Water transport properties of

601   cellophane flexible films intended for food packaging applications. *Journal of Food*

602   *Engineering*, *53*(4), 295–300. https://doi.org/10.1016/S0260-8774(01)00168-6

603   13. EFSA. (2007). Opinion of the Scientific Panel on Food Additives, Flavourings,

604   Processing Aids and Materials in Contact with Food on a request from the

605   Commission related to an application on the use of ethyl lauroyl arginate as a food

606   additive, LAMIRSA, 2008. *The EFSA Journal*, *511*, 1–27.

607   14. Figueroa-Lopez, K. J., Andrade-Mahecha, M. M., & Torres-Vargas, O. L. (2018).

608   Development of antimicrobial biocomposite films to preserve the quality of bread.

609   *Molecules*, *23*(1), 212. https://doi.org/10.3390/molecules23010212

610   15. Gaikwad, K. K., Lee, S. M., Lee, J. S., & Lee, Y. S. (2017). Development of

611   antimicrobial polyolefin films containing lauroyl arginate and their use in the

612   packaging of strawberries. *Journal of Food Measurement and Characterization*,

613   *11*(4), 1706–1716. https://doi.org/10.1007/s11694-017-9551-0

614   16. Gamarra, A., Missagia, B., Urpí, L., Morató, J., & Muñoz-guerra, S. (2018). Ionic

615   coupling of hyaluronic acid with ethyl *N*-lauroyl ₗ-arginate (LAE): Structure,

616   properties and biocide activity of complexes. *Carbohydrate Polymers*, *197*, 109–116.

617   https://doi.org/10.1016/j.carbpol.2018.05.057

618   17. Ghaderi, J., Hosseini, S. F., Keyvani, N., Gómez-Guillén, M. C. (2019). Polymer

619   blending effects on the physicochemical and structural features of the

620   chitosan/poly(vinyl alcohol)/fish gelatin ternary biodegradable films. *Food*

621   *Hydrocolloids,* 95, 122–132 https://doi.org/10.1016/j.foodhyd.2019.04.021

622   18. Gontard, N., Guilbert, S., & Cuq, J. (1992). Edible Wheat Gluten Films: Influence of

623   the Main Process Variables on Film Properties using Response Surface

624   Methodology. Journal of Food Science, 57(1), 190–195.

625   https://doi.org/10.1111/j.1365-2621.1992.tb05453.x

626   19. Haghighi, H., De Leo, R., Bedin, E., Pfeifer, F., Siesler, H. W., & Pulvirenti, A.

627   (2019a). Comparative analysis of blend and bilayer films based on chitosan and

628   gelatin enriched with LAE (lauroyl arginate ethyl) with antimicrobial activity for food

629   packaging applications. *Food Packaging and Shelf Life*, *19*, 31–39.

630   https://doi.org/10.1016/j.fpsl.2018.11.015

631   20. Haghighi, H., Biard, S., Bigi, F., Leo, R. De, Bedin, E., Pfeifer, F., Siesler, HW.,

632   Licciardello, F., Pulvirenti, A. (2019b). Comprehensive characterization of active

633   chitosan-gelatin blend films enriched with different essential oils. *Food Hydrocolloids*,

634   *95*, 33–42. https://doi.org/10.1016/j.foodhyd.2019.04.019

635   21. Hajji, S., Chaker, A., Jridi, M., Maalej, H., Jellouli, K., Boufi, S., & Nasri, M. (2016).

636   Structural analysis, and antioxidant and antibacterial properties of chitosan-poly (vinyl

637   alcohol) biodegradable films. *Environmental Science and Pollution Research*, *23* (15),

638   15310–15320. https://doi.org/10.1007/s11356-016-6699-9

639   22. Higueras, L., López-Carballo, G., Hernández-Muñoz, P., Gavara, R., & Rollini, M.

640   (2013). Development of a novel antimicrobial film based on chitosan with LAE (ethyl-

641   N$^{\alpha}$-dodecanoyl-L-arginate) and its application to fresh chicken. *International Journal*

642   *of Food Microbiology*, *165*(3), 339–345.

643   https://doi.org/10.1016/j.ijfoodmicro.2013.06.003

644   23. Jahan, F., Mathad, R. D., & Farheen, S. (2016). Effect of mechanical strength on

645   chitosan-pva blend through ionic crosslinking for food packaging application.

646   *Materials Today: Proceedings-Part B*, *3*(10), 3689–3696.

647   https://doi.org/10.1016/j.matpr.2016.11.014

648   24. Kanatt, S. R., Rao, M. S., Chawla, S. P., & Sharma, A. (2012). Active chitosan-

649   polyvinyl alcohol films with natural extracts. *Food Hydrocolloids*, *29*(2), 290–297.

650   https://doi.org/10.1016/j.foodhyd.2012.03.005

651   25. Kashiri, M., Cerisuelo, J. P., Domínguez, I., López-Carballo, G., Hernández-Muñoz,

652   P., & Gavara, R. (2016). Novel antimicrobial zein film for controlled release of lauroyl

653   arginate (LAE). *Food Hydrocolloids*, *61*, 547–554.

654   https://doi.org/10.1016/j.foodhyd.2016.06.012

655   26. Kim, J. H., Kim, J. Y., Lee, Y. M., & Kim, K. Y. (1992). Properties and swelling

656   characteristics of cross-linked poly (vinyl alcohol)/ chitosan blend membrane. *Journal*

657   *of Applied Polymer Science*, *45*(10), 1711–1717.

658   https://doi.org/10.1002/app.1992.070451004

659   27. Koosha, M., & Mirzadeh, H. (2015). Electrospinning, mechanical properties, and cell

660   behavior study of chitosan/PVA nanofibers. *Journal of Biomedical Materials Research*

661   *- Part A*, *103*(9), 3081–3093. https://doi.org/10.1002/jbm.a.35443

662   28. Kumar, S., Krishnakumar, B., Sobral, A. J. F. N., & Koh, J. (2019). Bio-based (

663   chitosan/PVA/ ZnO) nanocomposites film : Thermally stable and photoluminescence

664   material for removal of organic dye. *Carbohydrate Polymers*, *205*, 559–564.

665   https://doi.org/10.1016/j.carbpol.2018.10.108

666   29. Leceta, I., Guerrero, P., & De La Caba, K. (2013). Functional properties of chitosan-

667   based films. *Carbohydrate Polymers*, *93*(1), 339–346.

668   https://doi.org/10.1016/j.carbpol.2012.04.031

669   30. Leceta, I., Guerrero, P., Ibarburu, I., Dueñas, M. T., & De La Caba, K. (2013).

670   Characterization and antimicrobial analysis of chitosan-based films. *Journal of Food*

671   *Engineering*, *116*(4), 889–899. https://doi.org/10.1016/j.jfoodeng.2013.01.022

672   31. Liu, Y., Wang, S., & Lan, W. (2018). Fabrication of antibacterial chitosan-PVA

673   blended film using electrospray technique for food packaging applications.

674   *International Journal of Biological Macromolecules-Part A*, *107*, 848–854.

675   https://doi.org/10.1016/j.ijbiomac.2017.09.044

676   32. Ma, Q., Zhang, Y., & Zhong, Q. (2016). Physical and antimicrobial properties of

677   chitosan films incorporated with lauric arginate, cinnamon oil, and

678   ethylenediaminetetraacetate. *LWT - Food Science and Technology*, *65*, 173–179.

679   https://doi.org/10.1016/j.lwt.2015.08.012

680   33. Moreno, O., Cárdenas, J., Atarés, L., & Chiralt, A. (2017a). Influence of starch

681   oxidation on the functionality of starch-gelatin based active films. *Carbohydrate*

682   *Polymers*, *178*, 147–158. https://doi.org/10.1016/j.carbpol.2017.08.128

683   34. Moreno, O., Díaz, R., Atarés, L., & Chiralt, A. (2016). Influence of the processing

684   method and antimicrobial agents on properties of starch-gelatin biodegradable films.

685   *Polymer International*, *65*(8), 905–914. https://doi.org/10.1002/pi.5115

686   35. Moreno, O., Gil, À., Atarés, L., & Chiralt, A. (2017b). Active starch-gelatin films for

687   shelf-life extension of marinated salmon. *LWT - Food Science and Technology*, *84*,

688   189–195. https://doi.org/10.1016/j.lwt.2017.05.005

689   36. Muriel-Galet, V., Carballo, G. L., Hernández-Muñoz, P., & Gavara, R. (2016). Ethyl

690   Lauroyl Arginate (LAE): usage and potential in antimicrobial packaging. In J. Barros-

691   Velazquez (Ed), *Antimicrobial Food Packaging* (pp. 313–318). Academic Press.

692   https://doi.org/10.1016/B978-0-12-800723-5.00024-3

693   37. Muriel-Galet, López-Carballo, G., Gavara, R., & Hernández-Muñoz, P. (2015).

694   Antimicrobial effectiveness of lauroyl arginate incorporated into ethylene vinyl alcohol

695   copolymers to extend the shelf-life of chicken stock and surimi sticks. *Food and

696   Bioprocess Technology*, *8*(1), 208–217. https://doi.org/10.1007/s11947-014-1391-x

697   38. Muriel-Galet, V., López-Carballo, G., Hernández-Muñoz, P., & Gavara, R. (2014).

698   Characterization of ethylene-vinyl alcohol copolymer containing lauril arginate (LAE)

699   as material for active antimicrobial food packaging. *Food Packaging and Shelf Life*,

700   *1*(1), 10–18. https://doi.org/10.1016/j.fpsl.2013.09.002

701   39. Muriel-Galet, V., López-Carballo, G., Gavara, R., & Hernández-Muñoz, P. (2012).

702   Antimicrobial food packaging film based on the release of LAE from EVOH.

703   *International Journal of Food Microbiology*, *157*(2), 239–244.

704   https://doi.org/10.1016/j.ijfoodmicro.2012.05.009

705   40. Parida, U. K., Nayak, A. K., Binhani, B. K., & Nayak, P. L. (2011). Synthesis and

706   characterization of chitosan-polyvinyl alcohol blended with cloisite 30B for controlled

707   release of the anticancer drug curcumin. *Journal of Biomaterials and

708   Nanobiotechnology*, *2*, 414–425. https://doi.org/10.4236/jbnb.2011.24051

709   41. Pattanayaiying, R., H-Kittikun, A., & Cutter, C. N. (2015). Incorporation of nisin Z and

710   lauric arginate into pullulan films to inhibit foodborne pathogens associated with fresh

711 and ready-to-eat muscle foods. *International Journal of Food Microbiology*, *207*, 77–

712 82. https://doi.org/10.1016/j.ijfoodmicro.2015.04.045

713 42. Pavaloiu, R. D., Stoica-Guzun, A., Stroescu, M., Jinga, S. I., & Dobre, T. (2014).

714 Composite films of poly(vinyl alcohol)-chitosan-bacterial cellulose for drug controlled

715 release. *International Journal of Biological Macromolecules*, *68*, 117–124.

716 https://doi.org/10.1016/j.ijbiomac.2014.04.040

717 43. Pereira Jr, V. A., de Arruda, I. N. Q., & Stefani, R. (2015). Active chitosan/PVA films

718 with anthocyanins from *Brassica oleraceae* (Red Cabbage) as Time-Temperature

719 Indicators for application in intelligent food packaging. *Food Hydrocolloids*, *43*, 180–

720 188. https://doi.org/10.1016/j.foodhyd.2014.05.014

721 44. Rubilar, J. F., Candia, D., Cobos, A., Díaz, O., & Pedreschi, F. (2016). Effect of

722 nanoclay and ethyl-N$^\alpha$-dodecanoyl-*L*-arginate hydrochloride (LAE) on

723 physicomechanical properties of chitosan films. *LWT - Food Science and Technology*,

724 *72*, 206–214. https://doi.org/10.1016/j.lwt.2016.04.057

725 45. Sarwar, M. S., Niazi, M. B. K., Jahan, Z., Ahmad, T., & Hussain, A. (2018).

726 Preparation and characterization of PVA/nanocellulose/Ag nanocomposite films for

727 antimicrobial food packaging. *Carbohydrate Polymers*, *184*, 453–464.

728 https://doi.org/10.1016/j.carbpol.2017.12.068

729 46. Thakhiew, W., Devahastin, S., & Soponronnarit, S. (2013). Physical and mechanical

730 properties of chitosan films as affected by drying methods and addition of

731 antimicrobial agent. *Journal of Food Engineering*, *119*(1), 140–149.

732 https://doi.org/10.1016/j.jfoodeng.2013.05.020

733 47. Theinsathid, P., Visessanguan, W., Kruenate, J., Kingcha, Y., & Keeratipibul, S.

734 (2012). Antimicrobial activity of lauric arginate-coated polylactic acid films against

735 *Listeria monocytogenes* and *Salmonella* Typhimurium on cooked sliced ham. *Journal*

736 *of Food Science*, *77*(2), 142–149. https://doi.org/10.1111/j.1750-3841.2011.02526.x

737 48. Tripathi, S., Mehrotra, G. K., & Dutta, P. K. (2009). Physicochemical and bioactivity of

738 cross-linked chitosan–PVA film for food packaging applications. *International Journal*

739   *of*   *Biological*   *Macromolecules*,   *45(4)*,   372–376.

740   https://doi.org/10.1016/j.ijbiomac.2009.07.006

741   49. Tripathi, S., Mehrotra, G. K., & Dutta, P. K. (2008). Chitosan based antimicrobial films

742   for   food   packaging   applications.   *e-Polymers*.   *8*(1),   093.

743   https://doi.org/10.1515/epoly.2008.8.1.1082

744   50. USFDA. (2005). Center for Food Safety and Applied Nutrition, U.S. *Agency Response*

745   *Letter GRAS Notice No. GRN 000164.*

746   51. Wu, J., Sun, X., Guo, X., Ge, S., & Zhang, Q. (2017). Physicochemical properties,

747   antimicrobial activity and oil release of fish gelatin films incorporated with cinnamon

748   essential   oil.   *Aquaculture*   *and*   *Fisheries*,   *2*(4),   185–192.

749   https://doi.org/10.1016/j.aaf.2017.06.004

750   52. Yadav, M., & Chiu, F. C. (2019). Cellulose nanocrystals reinforced κ-carrageenan

751   based UV resistant transparent bionanocomposite films for sustainable packaging

752   applications.   *Carbohydrate*   *Polymers*,   *211*,   181–194.

753   https://doi.org/10.1016/j.carbpol.2019.01.114

Highlights:

- LAE was effectively incorporated into chitosan-polyvinyl alcohol films
- High LAE levels negatively affected mechanical and water barrier properties
- Addition of LAE improved UV barrier of chitosan-polyvinyl alcohol blend films
- The developed active films were effective against four food bacterial pathogens

Conflicts of Interest Statement

Manuscript title: Development of antimicrobial films based on chitosan-polyvinyl alcohol blend enriched with ethyl lauroyl arginate (LAE) for food packaging applications

The authors whose names are listed immediately below certify that they have NO affiliations with or involvement in any organization or entity with any financial interest (such as honoraria; educational grants; participation in speakers' bureaus; membership, employment, consultancies, stock ownership, or other equity interest; and expert testimony or patent-licensing arrangements), or non-financial interest (such as personal or professional relationships, affiliations, knowledge or beliefs) in the subject matter or materials discussed in this manuscript.

Author names:

1- Hossein Haghighi
2- Serge Kameni Leugoue
3- Frank Pfeifer
4- Heinz Wilhelm Siesler
5- Fabio Licciardello
6- Patrizia Fava
7- Andrea Pulvirenti

The authors whose names are listed immediately below report the following details of affiliation or involvement in an organization or entity with a financial or non-financial interest in the subject matter or materials discussed in this manuscript. Please specify the nature of the conflict on a separate sheet of paper if the space below is inadequate.

Author names:

This statement is signed by all the authors to indicate agreement that the above information is true and cor-rect (*a photocopy of this form may be used if there are more than 10 authors*):

Author's name (typed)	Author's signature	Date
Hossein Haghighi	*Hossein Haghighi*	9.7.2019
Serge Kameni Leugoue	*signature*	9.7.2019
Frank Pfeifer	*Frank Pfeifer*	23.07.2019
Heinz Wilhelm Siesler	*H. W. Siesler*	23.07.2019
Fabio Licciardello	*signature*	09.07.2019
Patrizia Fava	*Patrizia Fava*	09.07.2019
Andrea Pulvirenti	*signature*	9.7.2019